

Characterization of photochemical processes for H₂ production by CdS nanorod-[FeFe] hydrogenase complexes

Katherine A. Brown¹, Molly B. Wilker², Marko Boehm¹, Gordana Dukovic^{2*} and Paul W. King^{1*}

¹Biosciences Center, National Renewable Energy Laboratory, Golden CO 80401

²Department of Chemistry and Biochemistry, University of Colorado Boulder, Boulder, CO 80309

Ferredoxin expression and purification. The DNA sequence corresponding to the mature Ferredoxin (PetF) protein of *Chlamydomonas reinhardtii* was cloned into a modified pRSET-A expression vector.¹ The PCR fragment was amplified from the pMAPetF plasmid (kindly provided by Alexandra Dubini, National Renewable Energy Laboratory, USA) that contained a codon optimized version (Mr. Gene, USA) of the PetF cDNA using Phusion DNA polymerase (New England Biolabs, USA) and forward GGATCCTATAAAGTCACCTTGAAAACCCCATCCGG, and reverse GAATTCTCAATACAAGGCTTCTTCTTGATGGGTTTGAATT Fdx1 specific primers. After double digestion with EcoRI and BamHI, the fragment was ligated (Quick Ligation Kit, New England Biolabs, USA) into EcoRI/BamHI linearized pRSET-A vector. The resulting vector was transformed into KRX competent cells (Promega, USA).

For expression a 5-ml Terrific Broth (TB; VWR, USA) starter culture was grown overnight at 37 °C and diluted 1:100 in a 100-ml TB subculture the following morning. After the subculture had reached an OD₆₀₀ of ~0.4, 10 ml of it were used to inoculate a 1 L of TB media supplemented with 0.4% (w/v) glycerol. At an A₆₀₀ value of ~0.6, Rhamnose and Ferric ammonium citrate were added to final concentrations of 0.05% (w/v) and 2.5 mM respectively. The induced culture was then left for overnight incubation at RT on a shaker. The next day cells were harvested and resuspended in 50 ml lysis buffer (50 mM NaPO₄ pH=7.0, 300 mM NaCl, 5% (w/v) glycerol) to which one tablet of complete protease inhibitor (Roche, USA), 100 µl of 50 mg ml⁻¹ lysozyme (Sigma-Aldrich, USA) and 250 u of DNaseI (Thermo Scientific, USA) were added. The cells were then broken by two passages through a French Press cell (1200 psi; American Instrument Company, USA) and the cell lysate was incubated in a water bath for 15 min at 55°C. Subsequently, cell debris and precipitated protein was pelleted in an ultracentrifuge (Optima XL-100k ultracentrifuge, Beckman Coulter, USA) at 100,000xg and 4°C for 1 h. The supernatant was incubated for 1 h at 4°C with 10 ml of Talon metal affinity resin (Clontech Laboratories, USA). After the incubation period the resin was washed with 20 CV of lysis buffer, 10 CV of lysis buffer containing 10 mM imidazole and 10 CV of lysis buffer containing 20 mM imidazole. Protein elution was performed with 2 CV of lysis buffer containing 300 mM imidazole and eluted Ferredoxin was concentrated to a final volume of 2 ml using 5 kDa molecular weight cut-off (MWCO) concentrators (Satorius Stedim Biotech, USA). The 2-ml sample was then loaded on a HiLoad™ 26/60 Superdex™ 75 prep grade (GE Healthcare, USA) size exclusion column coupled to an Äkta FPLC (GE Healthcare, USA) and using 25 mM NaPO₄ pH=7.0, 100 mM NaCl, 5% (w/v) glycerol and 10 mM sodium dithionite as the running buffer at a flow rate of 2 ml min⁻¹. The run was monitored at an A₂₈₀ and the main peak eluted after approximately 195 ml. The pooled fractions (185 to 205 ml) were concentrated again and the final concentration was determined using the DC protein assay (Bio-Rad Laboratories, USA) according to the manufacturer's instructions.

CdS nanorod synthesis. 8.54 mmol trioctylphosphine oxide (TOPO; Sigma Aldrich, *ReagentPlus*®, 99%), 3.2 mmol n-octadecylphosphonic acid (ODPA; PCI Synthesis, 9 Opportunity Way, Newburyport, MA01950, 978-463-4853), and 1.61 mmol cadmium oxide (CdO; Sigma Aldrich, ≥99.99% trace metals basis) were stirred under vacuum at 120°C, then heated under Ar to 320°C, and held at that temperature for 1 h. Upon cooling to 120 °C, the mixture was evacuated for 1 h. Upon heating again to 320°C, 5.40 mmol tri-n-octylphosphine (TOP; Strem Chemicals, min. 97%), and 3.2 mmol Trioctylphosphine sulfide (TOP:S) were injected and nanocrystal growth proceeded for 45 min at 320°C. TOP:S was prepared by stirring TOP and elemental sulfur (Aldrich) in a 1:1 molar ratio at room temperature for 48 h. After cooling to 80°C, nanocrystals were precipitated with a toluene:acetone (1:2 volume ratio) mixture. Purification was performed by precipitation using toluene/octylamine/acetone (approximately 3:1:3 volume ratio) and chloroform/nonanoic acid/isopropanol mixtures. The nanocrystals were dissolved in hexane and the remaining impurities precipitated slowly. The final products were redispersed in toluene.

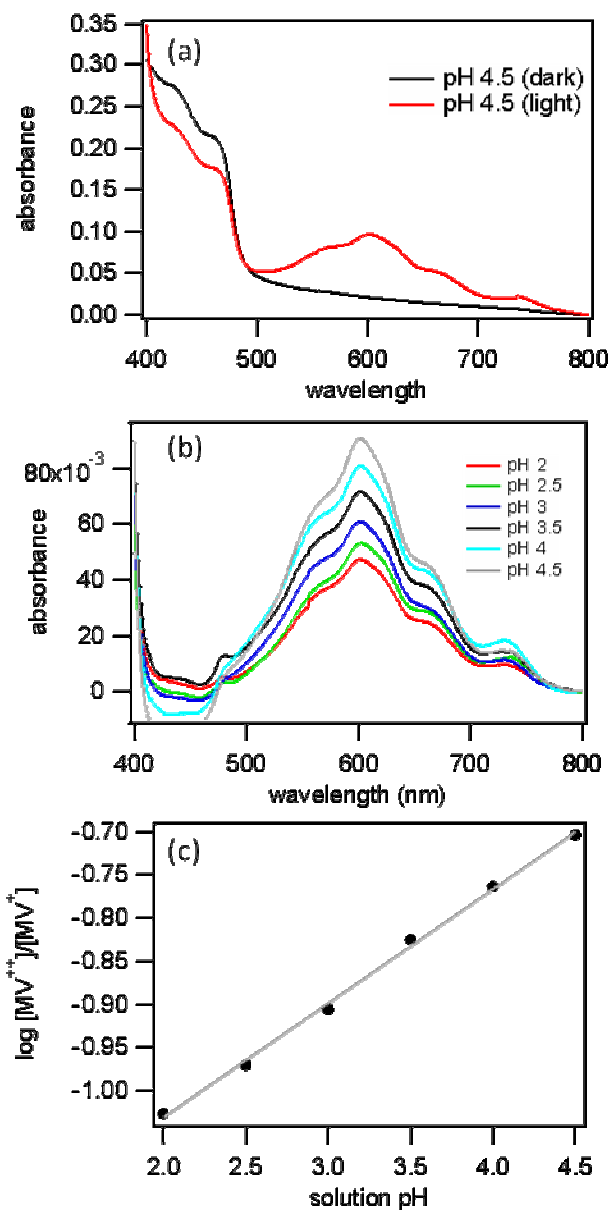


Figure S1. Determination of the reduction potentials of CdS nanorods. Mixtures of 83 nM MPA-CdS nanorods and 167 nM MV were combined under an anaerobic atmosphere of 4% H₂/96% N₂ in buffers of varying pH (2, 2.5, 3, 3.4, 4 and 4.5).^{2,3} Samples were illuminated for 10 min with 405 nm LED light at 800 uE m⁻² s⁻¹. (a) Absorbance spectra of pH 4.5 samples, before (black) and after (red) illumination. (b) Subtracted (illuminated – dark) spectra of CdS-MV solutions at pH values of 2, 2.5, 3, 3.4, 4 and 4.5. (c) Plot of the log [MV²⁺]/[MV⁺] vs pH. The MV⁺ concentrations were calculated based on absorbance at 606 nm and an $\epsilon=11000 \text{ M}^{-1} \text{ cm}^{-1}$ (path-length = 0.3 cm), and used to calculate MV²⁺ as $[\text{MV}^{2+}] = [\text{MV}^{\text{total}}] - [\text{MV}^+]$.

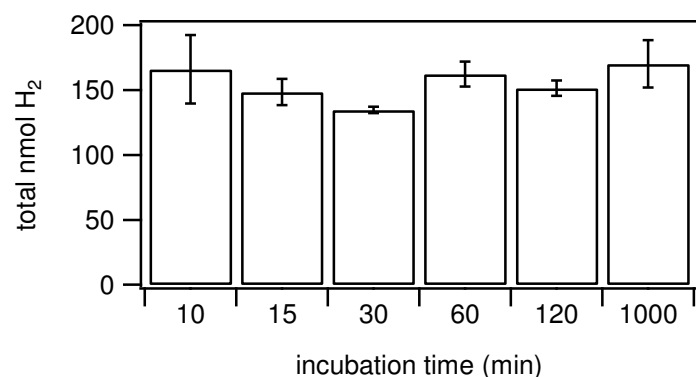


Figure S2. Time-dependence of photocatalytic activity for CdS:CaI mixtures. A 1:1 mixture of 92 nM CdS and 92 nM CaI was prepared in the dark and subsequently illuminated 10 min with white light ($10,000 \text{ uE m}^{-2} \text{ s}^{-1}$) at the specified time. Total nmol of H₂ in each reaction was measured by GC.

Table S1. Poisson distribution of CdS:CaI molar ratios present in various mixtures.

Molar Ratio of Mixture ^a	Bare ^b CdS	CdS:CaI Molar Ratio								
		1:1	1:2	1:3	1:4	1:5	1:6	1:7	1:8	1:9
1-to-5	0.01	0.03	0.08	0.14	0.18	0.18	0.15	0.10	0.07	0.04
1-to-2.5	0.08	0.21	0.26	0.21	0.13	0.07	0.03	0.01	0.00	0.00
1-to-1.33	0.26	0.35	0.23	0.10	0.03	0.01	0.00	0.00	0.00	0.00
1-to-0.67	0.51	0.34	0.11	0.03	0.00	0.00	0.00	0.00	0.00	0.00
1-to-0.33	0.72	0.24	0.04	0.00	0.00	0.00	0.00	0.00	0.00	0.00
1-to-0.167	0.85	0.14	0.01	0.00	0.00	0.00	0.00	0.00	0.00	0.00
1-to-0.083	0.92	0.08	0.00	0.00	0.00	0.00	0.00	0.00	0.00	0.00

^a Shown as ratio of CdS-to-CaI. It is expected that for CdS:CaI ratios that are greater than ~1:6 that steric factors (crowding) will affect the actual quantities of complexes within ratios >1:5. The Poisson distribution does not account these effects therefore the populations of ratios above 1:5 are included. Numbers represent the fraction of complexes at the specified coverage within the total CdS distribution.

^b nM.

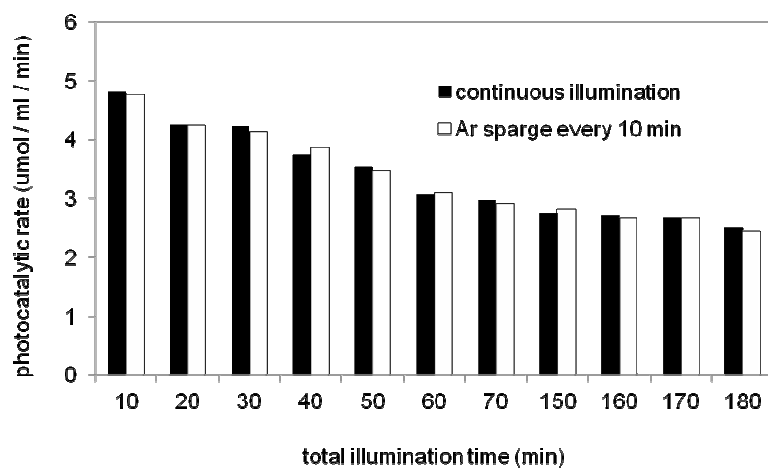


Figure S3. The effect of headspace H₂ on CdS:CaI photocatalytic rate. Solutions of 2:1 CdS:CaI, 24 nM CdS, 12 nM CaI were illuminated continuously (black bars) or in 10 min intervals with headspace replacement (white bars). The TOF of photocatalytic H₂ production ($\text{mol H}_2 \text{ mol}^{-1} \text{ CaI s}^{-1}$) was measured continuously during illumination in real time by an Omnistar capillary mass spectrometer (Pfeiffer, Germany).

Table S2. QY measurements for the 1-to-0.67 CdS-to-CaI complex.

Sample ^a	Incident power (mW)	Power absorbed (mW)	Absorbance ^b (t=0, min)	Absorbance ^b (t=10, min)	Photons absorbed (nmol)	H ₂ produced (nmol)	QY ^c (%)
1	0.97	0.13	0.13	0.14	262	28.7	21.9
2	1.03	0.14	0.13	0.14	287	28.9	20.2
3	0.97	0.17	0.15	0.16	352	33.6	19.1
4	1.27	0.19	0.15	0.15	383	38.9	20.3
5	1.01	0.20	0.16	0.16	411	41.1	20.0
6	1.02	0.19	0.15	0.16	386	41.5	21.5
7	1.07	0.20	0.15	0.15	403	39.7	19.7

^a Mixtures consisted of 14 nM CdS, 9nM CaI and 100 mM AA and were incubated for 10 min.

^b Incident and absorbed laser powers were measured at 0 and 10 min to rule out variations in laser intensity and changes in sample absorbance during the experiment.

^c QY= ([mol H₂ produced/mol photons absorbed]*[2 photons/mol H₂])*100%.

Table S3. Michaelis-Menten analysis of [AA]-dependence on photochemical H₂ production.

Kinetic Constant	Light Intensity ^a (405 nm, $\mu\text{E m}^{-2} \text{s}^{-1}$)	
	800	2000
K_M (mM)	1.3	4.9
k_{cat} (s ⁻¹)	83	192
k_{cat}/K_M (s ⁻¹ M ⁻¹)	6×10^4	4×10^4

^a Data from Figure 5a, normalized to the baseline values for 0 mM AA.

Table S4. TOF dependence of CdS:CaI complexes on molar ratio and light intensity.

Light intensity ($\mu\text{E m}^{-2} \text{s}^{-1}$)	TOF (s ⁻¹) ^a		Ratio 1-to-0.67/1-to- 0.083 ^b
	1-to-0.67	1-to-0.083	
800 (405 nm)	125	379	3.0
30,000 (white light)	291	983	3.4

^a TOF for each CdS-to-CaI ratio defined as, mol H₂ mol⁻¹ CaI s⁻¹.

^b The TOF of 1-to-0.083 divided by the TOF of 1-to-0.67.

Figure S4. UV-Vis absorption spectra of CdS:CaI complexes during long-term illumination. (a) UV-Vis absorption spectra of time-points during H₂ generation. Increasing absorbance due to AA oxidation is observed, with a new peak ~360 nm, and a

continuous background across the visible region.⁴ (b) Exciton peak intensity as a function of time. The peak intensity was estimated by subtracting the background from new AA oxidation products at 490 nm from the intensity at 472 nm. (There is no signal due to CdS at wavelengths to the red of 480 nm.) There is no significant change in CdS exciton intensity over time demonstrating a constant CdS concentration throughout the experiment. (c) Exciton peak position as a function of time, obtained by taking the second derivative of the absorption spectrum. The data shows no change in peak position, and therefore no decrease in CdS diameter. (d) Control experiment: UV-Vis absorption spectra of time-points during illumination of CdS solution in the presence of ascorbic acid and no CaI. Absorbance increase due to products of AA oxidation is not observed.

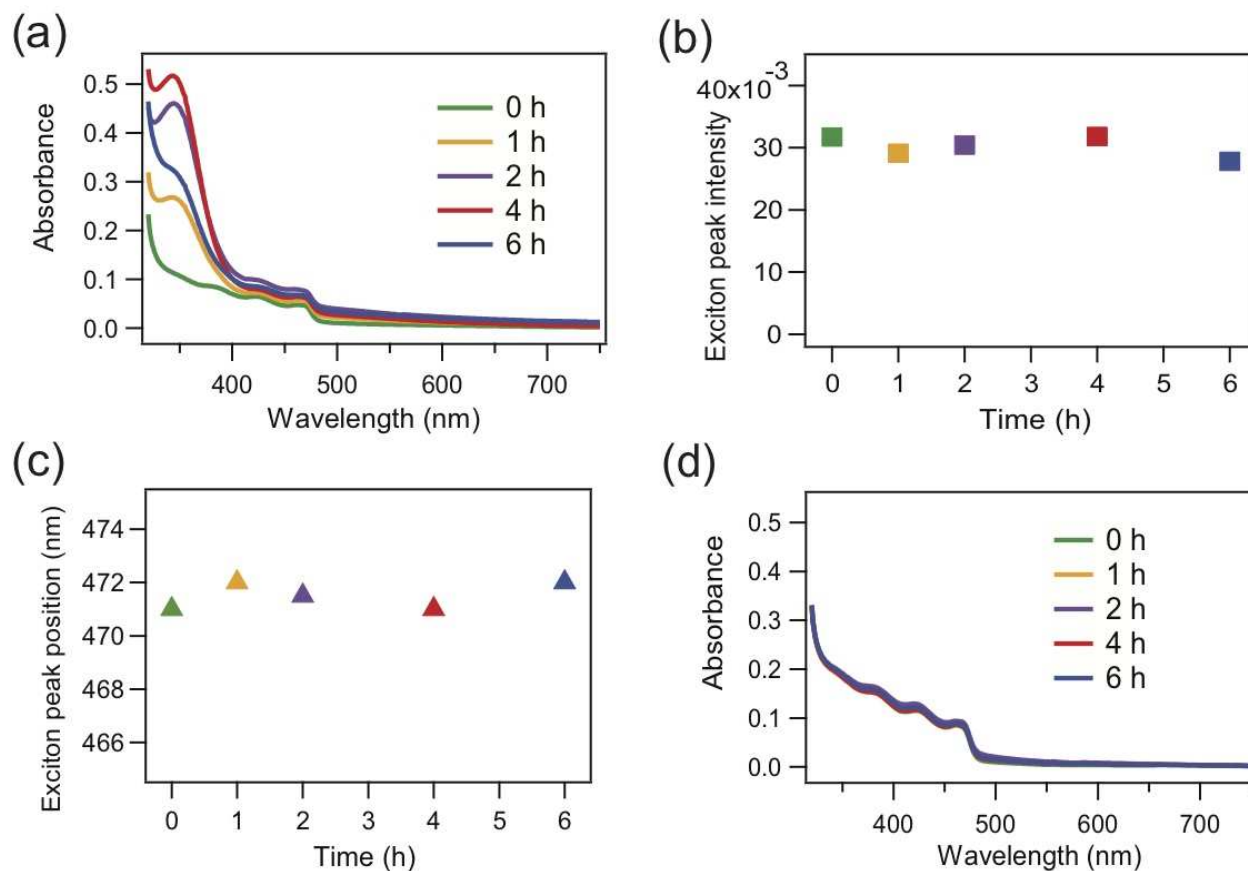


Figure S5. Analysis of TEM images at several time-points during long-term illumination. Distributions of CdS nanorod lengths and widths indicate no appreciable change in nanocrystal size during the first 2 h of illumination. It is not clear whether the apparent reduction in width at the 4 and 6 h time-points is statistically significant. CaI inactivation was 50 % complete within the first 2 h. This data demonstrates that CdS degradation is not the primary source of CaI inactivation.

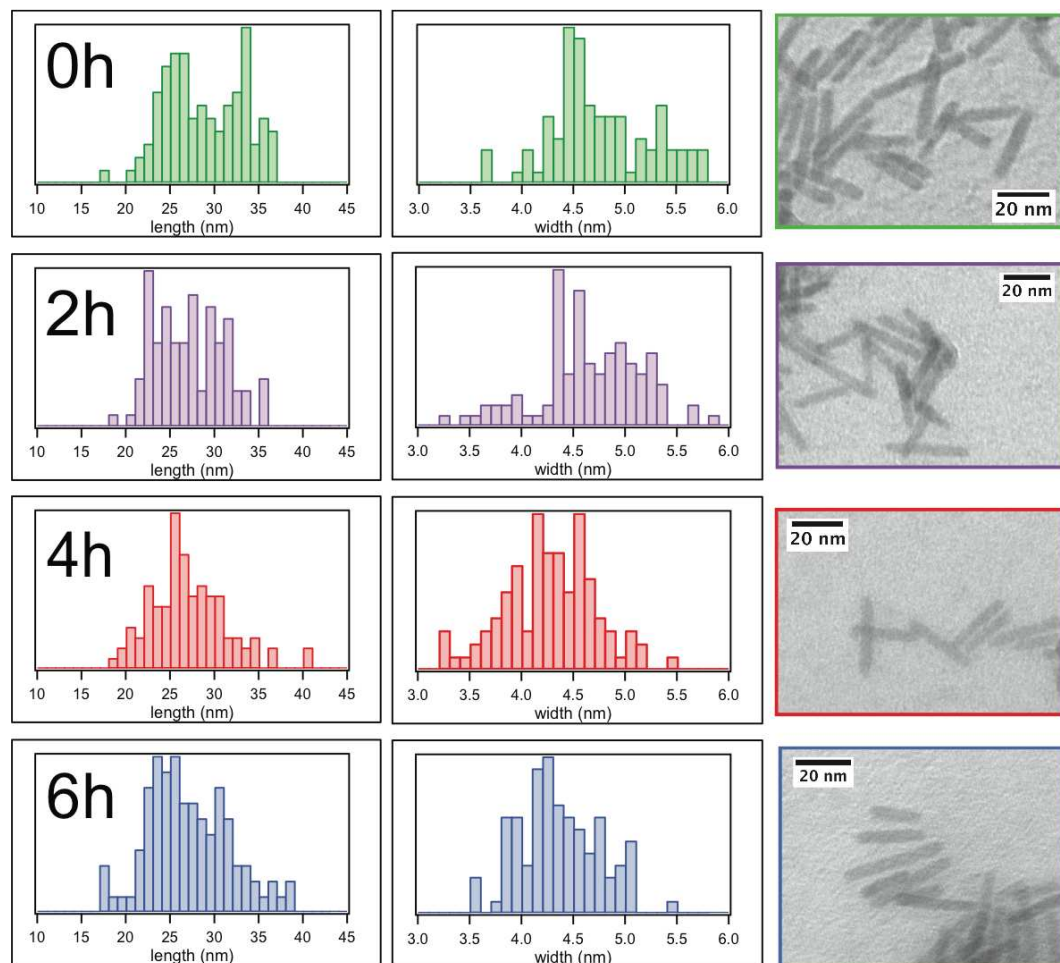
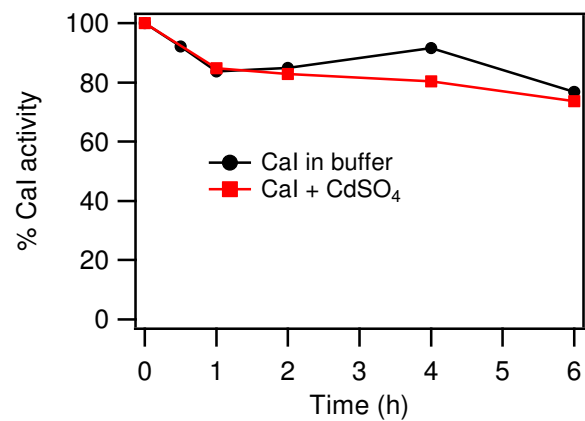


Figure S6. Effect of Cd^{2+} on CaI H_2 evolution activity. Reactions consisted of 38 nM CaI in 50 mM Tris-HCl, pH 7 buffer with (red squares) or without (black circles) 760 nM CdSO_4 . At each time-point a sample was taken and assayed for H_2 evolution activity from NaDT reduced MV (5 mM), and normalized to the activity at t_0 measured in the absence of CdSO_4 . The relative insensitivity of CaI to Ca^{2+} , in comparison to MPA sensitivity (Figure 6), further demonstrates that CdS degradation is not the cause of CaI inactivation.



References

- (1) Micboux, F.; Takasaka, K.; Boehm, M.; Nixon, P. J.; Murray, J. W. *Biochemistry* **2010**, *49*, 7411.
- (2) Dimitrijevic, N. M.; Savic, D.; Micic, O. I.; Nozik, A. J. *J. Phys. Chem.* **1984**, *88*, 4278.
- (3) Duonghong, D.; Ramsden, J.; Graetzel, M. *J. Am. Chem. Soc.* **1982**, *104*, 2977.
- (4) Bielski, B. H. J.; Allen, A. O.; Schwarz, H. A. *J. Am. Chem. Soc.* **1981**, *103*, 3516.